PROCEEDINGS OF SCIENCE

Recent measurements sensitive to PDFs

Qundong Han[a,*] **and on behalf of the ATLAS, CMS and LHCb Collaborations**

[a] *Central China Normal University,*
luoyu road 152, Wuhan, Hubei, China

E-mail: qundong.han@cern.ch

Parton Distribution Functions (PDFs) is an essential input for most of measurements at the Large Hadron Collider (LHC). And it is not be directly calculated and must be determined using experimental inputs which are Deep Inelastic Scattering (DIS) and hadron-hadron colliders. Many precision measurements are determined by the PDFs uncertainty. In this proceeding, the recent measurements sensitive to PDFs, using data collected in the LHC Run1 and Run2, are presented.

The Tenth Annual Conference on Large Hadron Collider Physics - LHCP2022
16-20 May 2022
online

*Speaker

PoS(LHCP2022)116

1. Introduction

At the LHC, ATLAS, CMS and LHCb are experiments that cover complementary phase-space to study electroweak process. Moreover, they can be used to probe Parton Distribution Functions and proton structure. LHC experiments provides measurements on a variety of PDF-sensitive standard candle processes with precision reaching a few percents. Their impact is subjected to possible tensions among different data and complications of the experimental systematic errors.

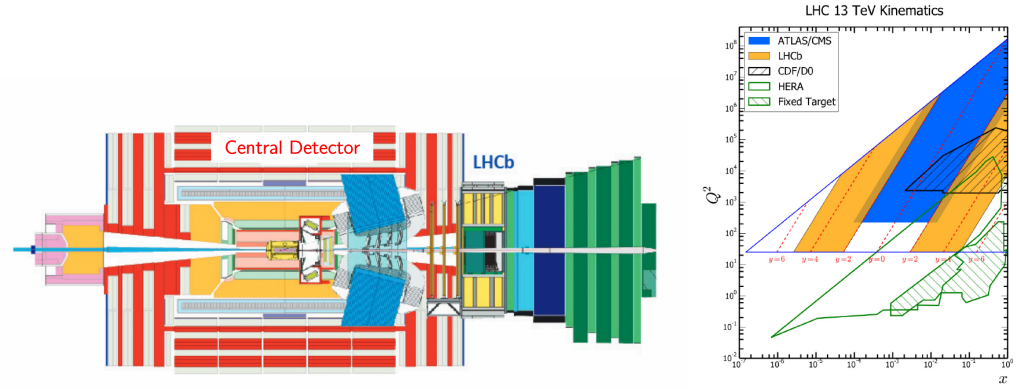

Figure 1: ATLAS, CMS and LHCb detector (left) and $x - Q^2$ plane showing the acceptance of several experiments (right), where x is the longitudinal momentum fraction of the proton carried by the parton and Q^2 is the energy scale of the interaction.

2. Measurement of forward Z production at $\sqrt{s} = 13$ TeV

LHCb performed precision measurement of forward Z boson production cross−section using $Z \to \mu^+\mu^-$decay in pp collisions at $\sqrt{s} = 13$ TeV, corresponding to an integrated luminosity of 5.1 fb^{-1} [3]. The measurement required events within the fiducial region defined as pseudorapidity $2.0 < \eta < 4.5$ and transverse momentum $p_T > 20$ GeV/c for both muons and dimuon invariant mass $60 < M_{\mu\mu} < 120\,\text{GeV}/c^2$. The determined integrated $Z \to \mu^+\mu^-$cross section is shown in Fig. 2, compared with the previous LHCb publication [4] and different theoretical predictions, including a prediction at next-to-next-to-leading order in perturbative quantum chromodynamics and a prediction with resummations. Measurements are in reasonable agreement with all theoretical predictions.

3. Measurement of Z + jets production at $\sqrt{s} = 13$ TeV

ATLAS performed the measurement of the production cross-section for a Z boson in association with high-transverse-momentum jets (p_T >100 GeV) and decaying into a charged lepton pair (e^+e^-, $\mu^+\mu^-$) production using pp collisions at $\sqrt{s} = 13$ TeV, corresponding to an integrated luminosity of 139 fb^{-1} [6]. Measurements of angular correlations between the Z boson and the closest jet are performed in events with at least one jet with $p_T \geq 500$ GeV. The measured cross sections are compared with theoretical predictions in Fig. 3.

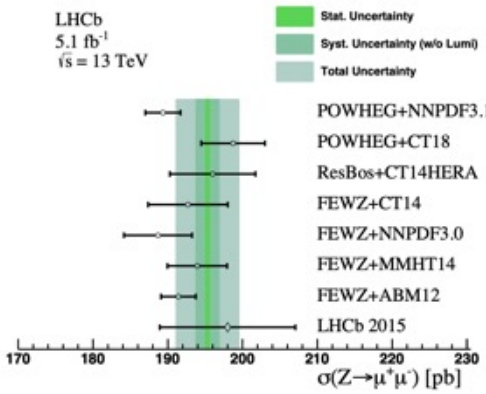

Figure 2: The integrated cross section compared with theoretical predictions.

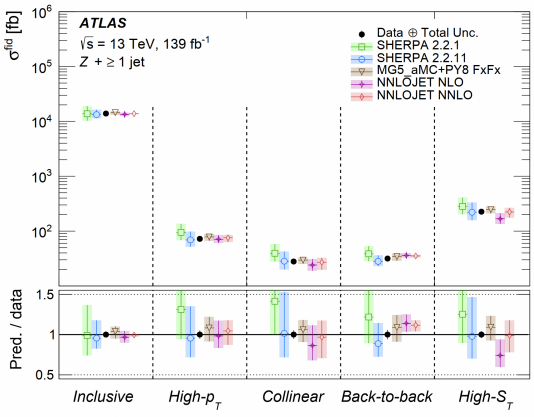

Figure 3: Differential integrated fiducial cross section compared with theoretical predictions.

CMS performed the measurement of the differential cross-sections for the production of a Z boson that decay into two electrons and muons in association with jets in pp collisions at $\sqrt{s} = 13$ TeV, corresponding to an integrated luminosity of 35.9 fb^{-1}[7]. The differential cross-sections are measured for Z bosons decaying to electrons and muons with transverse momentum $p_{\mathrm{T}} > 25\,\mathrm{GeV}$ and pseudorapidity $|\eta| < 2.4$ and at least one jet with $p_{\mathrm{T}} > 30\,\mathrm{GeV}$ and $|\eta| < 2.4$. The jet multiplicity distribution is measured for up to eight jets. All measurements are unfolded to the stable particle−level and compared with three theoretical predictions in Fig. 4.

4. Measurement of Z + b-jets production at $\sqrt{s} = 13$ TeV

CMS performed the measurement of the cross-section for the production of a Z boson, decaying to dielectrons and dimuons, in association with at least one bottom quark jet in pp collisions at $\sqrt{s} =$ 13 TeV, corresponding to an integrated luminosity of 137 fb^{-1}[8]. The integrated cross section for $Z + \geq 1$b jet and $Z + \geq 2$ b jets are measured for the electron, muon and combined channels. All measurements are compared with predictions from various event generators in Fig. 5.

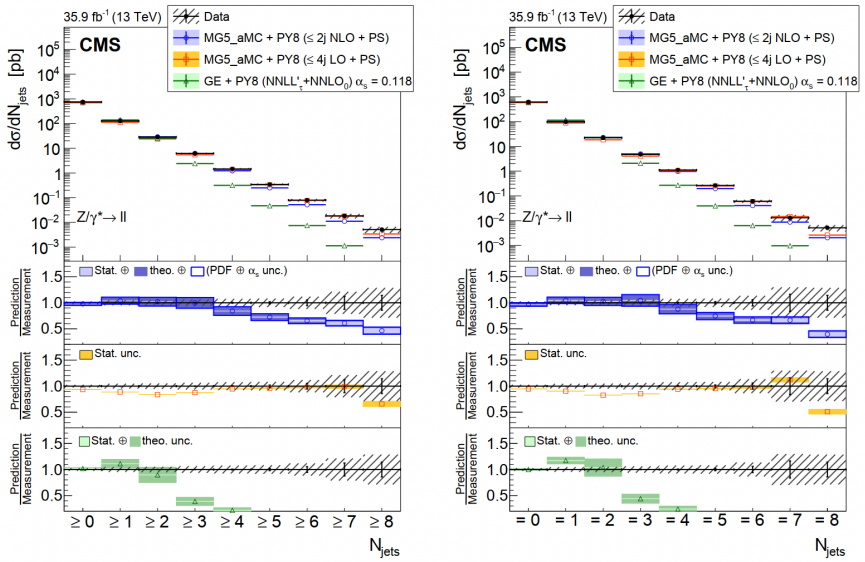

Figure 4: The measured differential cross-section as function of inclusive (left) and exclusive (right) jet multiplicities.

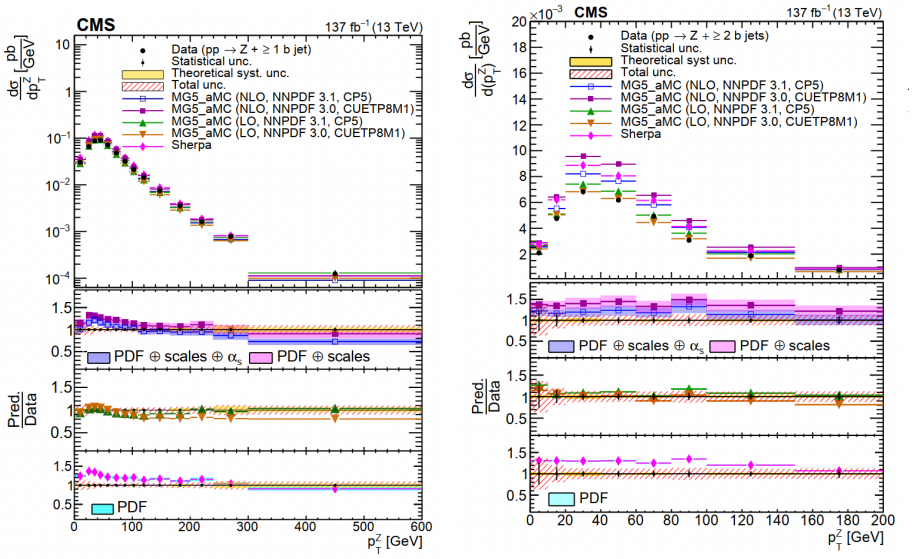

Figure 5: Differential cross-section distribution as a function of Z boson transverse momenta for Z + ≥1 b jet (left) and Z + ≥ 2 b jets (right).

5. Measurement of Z + c-jets production at $\sqrt{s}$ = 13 TeV

CMS measured differential cross-sections for Z bosons in association with at least one jet initiated by a charm quark in pp collisions at $\sqrt{s}$ = 13 TeV, corresponding to an integrated luminosity of 35.9 fb^{-1}[9]. The final states contain a pair of electrons or muons that are the decay

products of a Z boson, and a jet consistent with being initiated by a charm quark produced in the hard interaction. Differential cross-sections as a function of the transverse momentum p_{T} of the Z boson and p_{T} of the charm jet are compared with predictions from Monte Carlo event generators in Fig. 6.

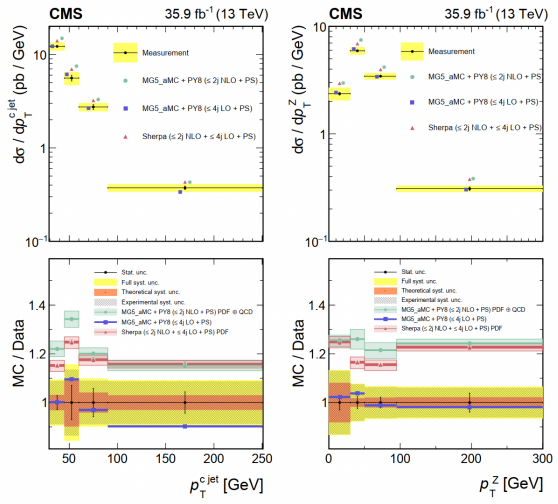

Figure 6: Measured fiducial differential cross-sections for inclusive Z + c jets production.

6. Measurement of Z boson in association with a flavour inclusive or double b-tagged large-radius jet at $\sqrt{s}$ = 13 TeV

ATLAS performed the cross-section measurement for production of a leptonically decaying Z boson in association with a large-radius jet in pp collisions at $\sqrt{s}$ = 13 TeV, corresponding to an integrated luminosity of 36 fb^{-1}[5]. Integrated and differential cross-sections are measured at particle-level in both flavour-inclusive and doubly b-tagged fiducial phase-spaces. The measurements are compared with current Monte Carlo predictions in Fig. 7.

7. Measurement and QCD analysis of double differential inclusive jet cross-sections at $\sqrt{s}$ = 13 TeV

CMS performed the measurement of double-differential inclusive jet cross sections in pp collisions at $\sqrt{s}$ = 13 TeV, corresponding to an integrated luminosity of 36.3(33.5) fb^{-1}[12]. The anti-k_T clustering algorithm is used with distance parameter of 0.4(0.7) in a phase space region with jet p_{T} from 97 GeV up to 3.1 TeV and $|y| < 2.0$. The measurement is used in a comprehensive QCD analysis at next-to-next-to-leading order, which results in significant improvement in the accuracy of the parton distributions in the proton. All predictions describe the data well within the experimental and theory uncertainties.

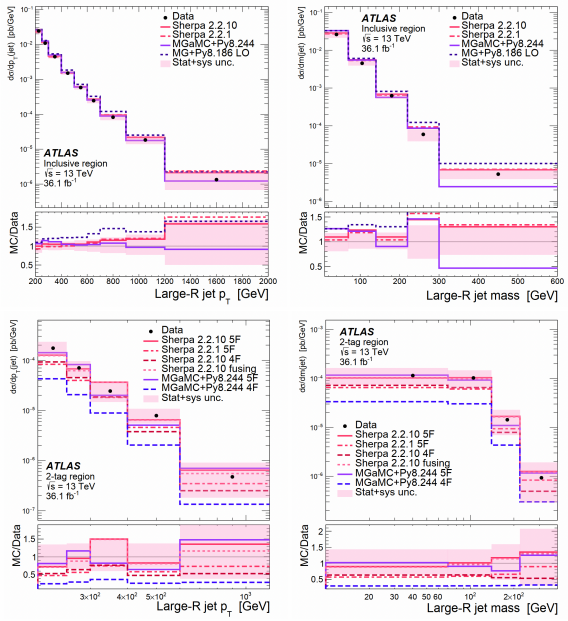

Figure 7: Particle-level differential cross-sections in inclusive event selection (top) and 2-tag event selection (bottom).

8. Intrinsic charm with Z bosons produced in association with charm jets

LHCb performed a study of Z bosons produced in association with charm in the forward region in pp collisions at $\sqrt{s} = 13$ TeV, corresponding to an integrated luminosity of 6 fb^{-1}[10]. The measurements show a hint of the intrinsic charm component in the high rapidity interval $(3.5 < y(Z) < 4.5)$ in Fig. 8.

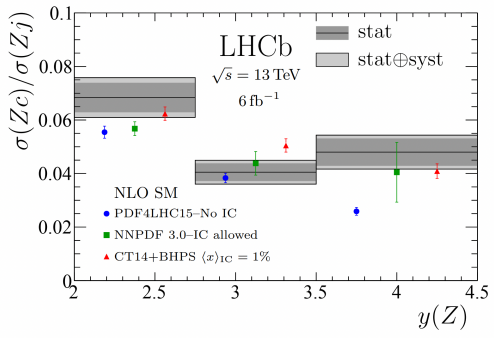

Figure 8: Measurements of $\sigma(Zc)/\sigma(Zj)$ in several pseudorapidity bins, compared to NLO SM predictions.

9. Measurements of the associated production of a W boson and a charm quark at $\sqrt{s}$ = 8 TeV

CMS performed measurements of the associated production of a W boson and a charm quark in pp collisions at $\sqrt{s}$ = 8 TeV, corresponding to an integrated luminosity 19.7 fb^{-1} [13]. The W bosons are identified through leptonic decays to an electron or a muon, and a neutrino. Charm quark jets are selected using distinctive signatures of charm hadron decays. The measurements are compared with theoretical predictions and slightly higher than MCFM NLO calculation with different PDF sets in Fig. 9.

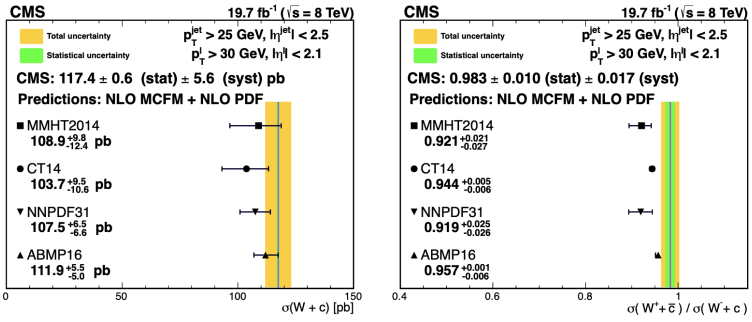

Figure 9: Comparison of the theoretical predictions for $\sigma(W + c)$ (left) and $\sigma(W^+ + \bar{c})/\sigma(W^- + c)$ (right) computed with MCFM and several sets of PDFs with the current experimental measurements.

10. First measurement of $Z \to \mu^+\mu^-$ angular coefficients in forward region at $\sqrt{s}$ = 13 TeV

LHCb firstly performed the study of the angular distribution of $\mu^+\mu^-$ pairs produced in the forward rapidity region via the Drell-Yan reaction $Z \to \mu^+\mu^-$ in pp collisions at $\sqrt{s}$ = 13 TeV, corresponding to an integrated luminosity 5.1 fb^{-1}[13]. At Born level, the angular distribution of the leptons in boson rest farm is given by

$$\frac{d\sigma}{d\cos\theta d\phi} \propto (1+\cos^2\theta) + \frac{1}{2}A_0(1-3\cos^2\theta) + A_1\sin 2\theta\cos\phi + \frac{1}{2}A_2\sin^2\theta\cos 2\phi + A_3\sin\theta\cos\phi + A_4\cos\theta + A_5\sin^2\theta\sin 2\phi + A_6\sin 2\theta\sin\phi + A_7\sin\theta\sin\phi, \quad (1)$$

where θ and ϕ are the polar and azimuthal angles of the μ^+ lepton in the Collins-Soper frame. The A_4 is sensitive to the weak mixing angle. In order to investigate its variation, the difference with respect to its mean value, ΔA_4, is measured. All muon candidates are required to have $p_T^\mu >$ 20 GeV/c and be in the range $2.0 < \eta < 4.5$. The relative uncertainty in the momentum of the muon track must be less than 10%. The total background contribution is determined to be 0.2%. The measured angular coefficients A_0 to A_3 as well as ΔA_4 and the difference A_0-A_2 are presented as a function of the Z boson p_T in Born level and the uncertainty is dominated by statistical uncertainty in Fig. 10.

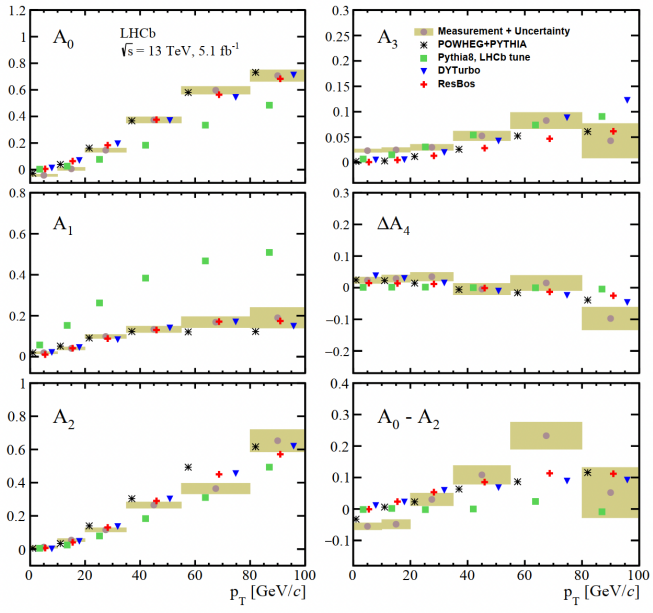

Figure 10: Comparison of the measured angular coefficients with different predictions.

11. Determination of PDFs using ATLAS data

ATLAS performed an analysis at next-to-next-to-leading order in the theory of quantum chromodynamics for the determination of a new set of proton parton distributions using diverse measurements in pp collisions at $\sqrt{s}$ = 7, 8 and 13 TeV, together with deep inelastic scattering data from ep collisions at collider[14]. The ATLAS data sets considered are differential cross section measurements of inclusive $W^{\pm}$ and Z boson production, $W^{\pm}$ and Z boson production in association with jets, $t\bar{t}$ production, inclusive jet production and direct photon production. In the analysis, particular attention is paid to the correction of systematic uncertainties within and between the various ATLAS data sets and to the impact of model, theoretical and parameterisation uncertainties. The resulting set of parton distribution functions is called ATLASpdf21.

12. Summary

LHC delivers plenty of PDF sensitive data with high statistics that have a significant impact on PDF extraction. LHC measurements start to dominate the global PDF fit results.

References

[1] CDF collaboration, *High-precision measurement of the W boson mass with the CDF II detector*, Science 376(2022)170.

[2] LHCb collaboration, *Measurement of the W boson mass*, JHEP01(2022)036.

[3] LHCb collaboration, *Precision measurement of forward Z boson production in proton-proton collisions at* $\sqrt{s} = 13$ *TeV*, JHEP07(2022)026.

[4] LHCb collaboration, *Measurement of the forward Z boson production cross-section in pp collisions at* $\sqrt{s} = 13TeV$, $JHEP09(2016)136$.

[5] ATLAS Collaboration, *Measurement of cross-sections for production of a Z boson in association with a flavor-inclusive or doubly b-tagged large-radius jet in proton-proton collisions at* $\sqrt{s} = 13$ *TeV with the ATLAS experiment*, arXiv:2204.12355.

[6] ATLAS Collaboration, *Cross-section measurements for the production of a Z boson in association with high-transverse-momentum jets in pp collisions at* $\sqrt{s} = 13$ *TeV with the ATLAS detector*, arXiv:2205.02597.

[7] CMS Collaboration, *Measurement of differential cross sections for the production of a Z boson in association with jets in proton-proton collisions at* $\sqrt{s} = 13$ *TeV*, arXiv:2205.02872.

[8] CMS Collaboration, *Measurement of the production cross section for Z + b jets in proton-proton collisions at* $\sqrt{s} = 13$ *TeV*, PhysRevD.105.092014.

[9] ATLAS Collaboration, *Measurement of differential cross sections for Z bosons produced in association with charm jets in pp collisions at* $\sqrt{s} = 13TeV$, $JHEP04(2021)109$.

[10] LHCb Collaboration, *Study of Z Bosons Produced in Association with Charm in the Forward Region*, PhysRevLett.128.082001.

[11] CMS Collaboration, *Measurements of the associated production of a W boson and a charm quark in proton-proton collisions at* $\sqrt{s} = 8$ *TeV*, arXiv:2112.00895.

[12] CMS Collaboration, *Measurement and QCD analysis of double-differential inclusive jet cross sections in proton-proton collisions at* $\sqrt{s} = 13TeV$, $JHEP02(2022)142$.

[13] LHCb Collaboration, *First Measurement of the* $Z \to \mu^+\mu^-$ *Angular Coefficients in the Forward Region of pp Collisions at* $\sqrt{s} = 13$ TeV, PhysRevLett.129.091801.

[14] CMS Collaboration, *Determination of the parton distribution functions of the proton using diverse ATLAS data from pp collisions at* $\sqrt{s}$*=7, 8 and 13 TeV*, Eur.Phys.J.C82,438(2022).